Time-of-Use and Demand Charge Battery Controller using Stochastic Model Predictive Control

Preprint

Michael Blonsky,[1] Killian McKenna,[1] Tyrone Vincent,[2] and Adarsh Nagarajan[1]

[1] *National Renewable Energy Laboratory*
[2] *Colorado School of Mines*

Presented at the IEEE International Conference on Communications, Control, and Computing Technologies for Smart Grids (IEEE SmartGridComm) November 11–13, 2020

NREL is a national laboratory of the U.S. Department of Energy
Office of Energy Efficiency & Renewable Energy
Operated by the Alliance for Sustainable Energy, LLC

This report is available at no cost from the National Renewable Energy Laboratory (NREL) at www.nrel.gov/publications.

Contract No. DE-AC36-08GO28308

Conference Paper
NREL/CP-5D00-76240
November 2020

Time-of-Use and Demand Charge Battery Controller using Stochastic Model Predictive Control

Preprint

Michael Blonsky,[1] Killian McKenna,[1] Tyrone Vincent,[2] and Adarsh Nagarajan[1]

[1] *National Renewable Energy Laboratory*
[2] *Colorado School of Mines*

Suggested Citation
Blonsky, Michael, Killian McKenna, Tyrone Vincent, and Adarsh Nagarajan. 2020. *Time-of-Use and Demand Charge Battery Controller using Stochastic Model Predictive Control: Preprint*. Golden, CO: National Renewable Energy Laboratory. NREL/CP-5D00-76240. https://www.nrel.gov/docs/fy21osti/76240.pdf.

NREL is a national laboratory of the U.S. Department of Energy
Office of Energy Efficiency & Renewable Energy
Operated by the Alliance for Sustainable Energy, LLC

This report is available at no cost from the National Renewable Energy Laboratory (NREL) at www.nrel.gov/publications.

Contract No. DE-AC36-08GO28308

Conference Paper
NREL/CP-5D00-76240
November 2020

National Renewable Energy Laboratory
15013 Denver West Parkway
Golden, CO 80401
303-275-3000 • www.nrel.gov

NOTICE

This work was authored in part by the National Renewable Energy Laboratory, operated by Alliance for Sustainable Energy, LLC, for the U.S. Department of Energy (DOE) under Contract No. DE-AC36-08GO28308. Funding provided by U.S. Department of Energy Office of Energy Efficiency and Renewable Energy. The views expressed herein do not necessarily represent the views of the DOE or the U.S. Government.

Cover Photos by Dennis Schroeder: (clockwise, left to right) NREL 51934, NREL 45897, NREL 42160, NREL 45891, NREL 48097, NREL 46526.

Time-of-use and Demand Charge Battery Controller Using Stochastic Model Predictive Control

Michael Blonsky*†, Killian McKenna*, Tyrone Vincent†, and Adarsh Nagarajan*
*National Renewable Energy Laboratory, Golden, Colorado
†Electrical Engineering, Colorado School of Mines, Golden, Colorado
Email: michael.blonsky@nrel.gov

***Abstract*—Stationary batteries in residential and commercial buildings are often used to smooth customer load profiles and to lower customer electricity bills. Controllers for these battery systems should account for customer energy consumption, rate structures, and high internal battery temperatures, which can lead to reduced performance over the battery lifetime. It is important to consider the uncertainty in forecasting energy consumption and temperature, especially for customers with highly variable and uncertain loads. We propose a novel battery controller using stochastic model predictive control that accounts for these uncertainties and can handle complex rate structures, including demand charges. We show that the controller performs better than standard model predictive control when there is significant uncertainty in the forecast. We also show improvements in the performance with more accurate forecasts and with a more aggressive control strategy.**

I. Introduction

The U.S. residential battery market more than doubled in 2019 and is expected to triple in 2020, and non-residential behind-the-meter batteries increased by 38% in 2019 [1]. Market growth is primarily driven by decreasing battery costs and new rate structures that allow customers to monetize the value of the battery [2]. This is often done through one of three mechanisms: self-consumption of on-site generation to reduce energy imports, energy arbitrage to import energy at low price times and export at high price times, and demand charge reduction by reducing the maximum imported demand [3].

Controllers decide when to charge and discharge the battery. They typically depend on the customer's rate structure, which may include time-based rates, demand charges, and feed-in tariffs. Optimal control often depends on the customer's electricity consumption (and solar production if it exists), which can be highly variable and uncertain. Batteries also experience capacity degradation due to fast cycling and high temperatures, which may be significant if batteries are installed outside or in unconditioned spaces [4].

Numerous studies have developed battery models to better understand the impacts of battery cycling, temperature, and other conditions on battery performance and degradation. Detailed models for specific battery chemistries and configurations include many chemical, electrical, and thermal parameters [5], [6]. Many papers use lumped models for packaged battery products and general applications. Some models include a 1- or 2-node thermal model to track internal battery temperatures [7]–[9].

There are also numerous battery controllers in the literature that are designed for maximizing economic output of the battery. Simple controllers have a time-based schedule based on a rate structure. Others are load-following to achieve maximum self-consumption or minimum grid import and/or export [10]. More complex controllers calculate when to charge and discharge using a heuristic algorithm [7] or through optimization that involves the load profile and rate structure. Many papers use model predictive control (MPC) to account for future load and rate changes in the current control decision [11]–[13].

Because residential and commercial consumption is often highly variable and uncertain, MPC controllers may not be well-suited for these applications. For example, a peak-shaving controller may be able to flatten a load profile given a perfect forecast of future demand; however, if the actual consumption is very different from the forecast, it is unlikely to fully flatten the peak. For systems with significant uncertainty in their forecasts, the assumptions from MPC may lead to sub-optimal decisions.

Stochastic Model Predictive Control (SMPC) resolves these issues by accounting for uncertainty in the control problem. SMPC is similar to MPC in that it solves an optimal control problem on a receding time horizon, but the underlying model includes stochastic disturbances and measurement error [14]. SMPC has been used in many energy applications [15]–[17]. [18] uses SMPC for stationary batteries at the utility-scale level with objectives that are not as relevant at the customer level.

We propose a stochastic model predictive controller for customer-sited, behind-the-meter batteries that incorporates uncertainty in customer load and ambient temperature. The controller minimizes costs based on time-of-use and demand charge rate structures and operational costs due to degradation. The key contributions of this paper include the integration of a thermo-electric battery model, a stochastic model predictive controller to minimize customer energy costs and battery degradation, and a demand charge in the SMPC optimization.

In Section II, we formulate the battery model and the SMPC optimization problem for the battery controller. In Section III, we use residential customer AMI data to show the benefits of the controller and the importance of understanding risk and uncertainty in this application. We conclude by presenting ideas for SMPC in related energy applications.

II. Formulation

A. Model Formulation

A linear battery model was used to keep the SMPC optimization problem solvable and computationally efficient. The electrical model is a common model taken from [11]. It tracks the battery state-of-charge as:

$$\frac{dSOC}{dt} = \eta_b \eta_i P_{\text{chg}} - \frac{1}{\eta_b \eta_i} P_{\text{dis}} \tag{1}$$

where SOC is the battery state-of-charge, P_{chg} is the AC charging power, P_{dis} is the AC discharging power, η_b is the battery efficiency, and η_i is the inverter efficiency. Note that the efficiencies are the same for charging and discharging.

The thermal model is a lumped model that has also been used elsewhere for batteries [7]. It tracks the battery internal temperature as:

$$\frac{dT_b}{dt} = \frac{1}{C_{\text{th}}} \left((1-\eta_b) P_{\text{chg}} + \frac{1-\eta_b}{\eta_b} P_{\text{dis}} + \frac{T_a - T_b}{R_{\text{th}}} \right) \tag{2}$$

where T_b is the battery temperature, T_a is the ambient temperature, R_{th} is the thermal resistance, and C_{th} is the thermal mass. External heat gains are not included in the model.

The electrical and thermal models combine to create a 2-state, fully observable state space model of the form:

$$\begin{aligned} \dot{x} &= A_c x + B_c u + G_c z \\ y &= x \end{aligned} \tag{3}$$

where:

$$x = \begin{bmatrix} SOC \\ T_b \end{bmatrix}, u = \begin{bmatrix} P_{\text{chg}} \\ P_{\text{dis}} \end{bmatrix}, z = \begin{bmatrix} T_a \\ P_{\text{load}} \end{bmatrix}$$

and A_c, B_c, and G_c are defined from Equations (1) and (2). Note that u is a vector of controllable inputs, and z is a vector of non-controllable inputs.

We then discretize the model assuming piece-wise constant inputs at a sampling time of T_s, provide a probabilistic model for the non-controllable inputs z, and add measurement noise to the outputs y. We denote a random sequence with a tilde, e.g. $\tilde{z}$, and its expected value as $\overline{z} = E[\tilde{z}]$. The final linear model is:

$$\begin{aligned} \tilde{x}_{k+1} &= A\tilde{x}_k + Bu_k + G\tilde{z}_k \\ \tilde{y}_k &= \tilde{x}_k + \tilde{v} \end{aligned} \tag{4}$$

where:

$$\begin{aligned} A &= e^{A_c T_s} \\ B &= A_c^{-1}(A - I)B_c \\ G &= A_c^{-1}(A - I)G_c \end{aligned}$$

The signals $\tilde{z}$ and $\tilde{v}$ are modeled as independent random sequences with a multivariate Gaussian distribution. The density of non-controllable inputs $\tilde{z}_k \sim \mathcal{N}(\overline{z}_k, Q_{z,k})$ varies with time. The density of measurement noise $\tilde{v} \sim \mathcal{N}(0, Q_v)$ does not vary with time. We assume $Q_{\tilde{z},k}$ is a diagonal matrix and define its elements as $\sigma^2_{T_a,k}$ and $\sigma^2_{P_{\text{load}},k}$, representing the time-varying variance of the non-controllable loads $T_{a,k}$ and $P_{\text{load},k}$.

Under these assumptions, the states have a Gaussian distribution with a density $\tilde{x}_k \sim \mathcal{N}(\overline{x}_k, Q_{x,k})$. The diagonal elements of $Q_{x,k}$ are defined as $\sigma^2_{SOC,k}$ and $\sigma^2_{T_b,k}$. Using the Kalman filter equations for time and measurement updates [19], the parameters of the state density are given by:

$$\begin{aligned} \overline{x}_k &= \overline{x}_k^- + K(y_k - \overline{x}_k^-) \\ Q_{x,k} &= Q_{x,k}^-(I - K) \end{aligned} \tag{5}$$

where:

$$\begin{aligned} K &= Q_{x,k}^-(Q_{x,k}^- + Q_v)^{-1} \\ \overline{x}_{k+1}^- &= A\overline{x}_k + Bu_k + G\overline{z}_k \\ Q_{x,k+1}^- &= AQ_{x,k}A^T + GQ_{z,k}G^T \end{aligned} \tag{6}$$

Note that the above equations can be used iteratively to calculate the density of states further in the future than $\tilde{x}_{k+1}$. When the measurement y_k is unknown, we set $\overline{x}_k = \overline{x}_k^-$.

For calculating demand charges, we track the peak power of the battery and load:

$$P_{\text{peak},k} = \max(P_{\text{tot},k}, P_{\text{peak},k-1}) \tag{7}$$

$$\tilde{P}_{\text{tot},k} = P_{\text{chg},k} - P_{\text{dis},k} + \tilde{P}_{\text{load},k} \tag{8}$$

Note that $\tilde{P}_{\text{load},k}$ is a random sequence when $k > 0$ and therefore $\tilde{P}_{\text{tot},k}$ is a random sequence with the same variance as $\tilde{P}_{\text{load},k}$. We define a deterministic form of Equation (8) using $\overline{P}_{\text{load},k}$ and $\overline{P}_{\text{tot},k}$. In our formulation, we do not calculate $P_{\text{peak},k}$ when $k > 0$.

B. Controller Formulation

The battery controller is designed to minimize battery costs while keeping the battery state x within reasonable constraints. The controller uses a SMPC framework that accounts for the uncertainty in state variables $\tilde{x}_k$ and in non-controllable inputs $\tilde{z}_k$. The variance of these values is used in the objective function and in the constraints of the optimization problem. The horizon length is n_k and the total horizon time is $T_s n_k$.

The objective function used in this paper consists of 5 terms. The first two terms capture costs associated with a time-based rate and a demand charge, respectively. The second two terms capture lifetime degradation costs associated with power and temperature. Quadratic relationships for power are used to estimate the increased degradation at large charge and discharge currents. The final term captures the future benefit for maintaining charge in the battery at the end of the horizon.

$$\begin{aligned} J = &\sum_{k=1}^{n_k} c_{\text{tou},k} T_s \overline{P}_{\text{tot},k} \\ &+ c_{\text{peak}} \max_{k \in [1,n_k]} \left(\overline{P}_{\text{tot},k} - P_{\text{peak},0} + \zeta_P \sigma_{P_{\text{load},k}}, 0 \right) \\ &+ \beta_P \sum_{k=1}^{n_k} \left(P^2_{\text{chg},k} + P^2_{\text{dis},k} \right) \\ &+ \beta_T \sum_{k=1}^{n_k} \max \left(\overline{T}_{b,k} - T_{\text{high}}, 0 \right)^2 \\ &+ c_{\text{tou},n_k} \eta_b \eta_i \overline{SOC}_{n_k} \end{aligned} \tag{9}$$

where J is the total cost, $c_{\text{tou},k}$ is the time-of-use rate at sample k, c_{peak} is the demand charge rate, and ζ_P, β_P, β_T, and T_{high} are tuning parameters that adjust the relative costs and

risks of high net loads, high battery power, and high battery temperatures. We assume the electricity price $c_{\text{tou},k}$ is net-energy metered. The 2nd term includes a back-off magnitude $\zeta_P \sigma_{P_{\text{load},k}}$ to account for the risk of variability in $\overline{P}_{\text{tot},k}$ (see [14]). We note that the cost function will only account for the incremental increase in the demand charge across the horizon.

There is no uncertainty in the power inputs or in any other parameter in the electrical model, so SOC is a deterministic state. Therefore, P_{chg}, P_{dis}, and SOC can be bounded with hard constraints:

$$\begin{aligned} P_{\text{chg},k} &\geq 0 && \forall k \in [1, n_k] \\ P_{\text{dis},k} &\geq 0 && \forall k \in [1, n_k] \\ SOC_{\min} \leq \overline{SOC}_k &\leq SOC_{\max} && \forall k \in [1, n_k] \end{aligned} \tag{10}$$

where $SOC_{\min}$ is the reserve SOC of the battery, and $SOC_{\max}$ is the battery capacity.

The battery temperature $\tilde{T}_b$ is a random variable due to the stochastic nature of $\tilde{T}_a$, and must be bounded using a chance constraint to ensure that the battery operates at a safe temperature and to limit the risk of thermal run-away:

$$\overline{T}_{b,k} \leq T_{\max} - \zeta_T \sigma_{T_b,k} \ \forall k \in [1, n_k] \tag{11}$$

where $\overline{T}_{b,k}$ is the controller's estimated value of $T_{b,k}$, $T_{\max}$ is a soft constraint of maximum temperature and $\zeta_T \sigma_{T_a,k}$ is the back-off magnitude (see [14]). Note that $T_{\max}$ is not necessarily the same as T_{high}, but both terms ensure low battery temperatures.

Finally, the linear model from (4) provides equality constraints for states across the time horizon:

$$\overline{x}_k = A\overline{x}_{k-1} + Bu_{k-1} + G\overline{z}_{k-1} \ \forall k \in [1, n_k] \tag{12}$$

Combining Equations (9-12) gives the final control problem:

$$\begin{aligned} (P_1) \min_{u_k} : \quad & J \\ \text{s.t.} \quad & u_k \geq 0 \\ & SOC_{\min} \leq \overline{SOC}_k \leq SOC_{\max} \\ & \overline{T}_{b,k} \leq T_{\max} - \zeta_T \sigma_{T_b,k} \\ & \overline{x}_k = A\overline{x}_{k-1} + Bu_{k-1} + G\overline{z}_{k-1} \\ & \forall k \in [1, n_k] \end{aligned} \tag{13}$$

We note that $\overline{z}_k$ and $Q_{z,k}$ are required inputs for P_1 for the entire horizon. The state variance $\sigma^2_{T_b,k}$ can also be pre-computed using Equations (5) and (6).

All constraints are linear, and the objective function is strictly convex (when assuming reasonable values for some parameters, e.g. all $\beta > 0$), making P_1 a convex optimization problem that guarantees a globally optimum solution and can be solved efficiently. The formulation also ensures that P_{chg} and P_{dis} are never non-zero at the same time step when $c_{\text{tou}} > 0$ and $0 < \eta_b \eta_i < 1$ (see [11]).

III. Results

We test the battery model and controller described in Section II and assess the control performance in multiple scenarios. Two reference scenarios test an MPC controller with a perfect forecast and with a forecast with high uncertainty. SMPC scenarios test the control performance by varying the level of risk and forecast uncertainty. All scenarios are run for a single residential customer with high PV generation over a 1-month period. The simulations are run at 30-minute time intervals, and the horizon is 24 hours, or 48 time steps.

TABLE I. Model and Control Parameters Used for Scenarios

Parameter	Value
P_{load} and $\sigma^2_{P_{\text{load}},k}$	varies, see Figure 1
T_a and $\sigma^2_{T_a,k}$	varies, see Figure 1
η_b	98 %
η_i	97 %
C_{th}	90 kJ/K
R_{th}	60 K/kW
Q_v	$\begin{bmatrix} 0.05\text{ kW} & 0 \\ 0 & 1^\circ\text{C} \end{bmatrix}$
T_s	30 minutes
n_k	48
c_{tou}	Off-peak: 0.012376 \$/kWh Shoulder: 0.026377 \$/kWh On-peak: 0.123296 \$/kWh
c_{peak}	8.5674 \$/kW
β_P	0.001
β_T	0.002
ζ_P	2.33 (99th percentile)
ζ_T	2.33 (99th percentile)
T_{high}	30 °C
$T_{\max}$	40 °C
$SOC_{\min}$	0 kWh
$SOC_{\max}$	10 kWh

All scenarios use parameter values described in Table I unless otherwise noted. The load profile was taken from an open-source dataset of residential customers with rooftop PV near Sydney, Australia [20]. We used data over a month for a single customer with high energy consumption, a high PV capacity of 4.5 kW, and no controllable loads. The temperature profile was taken from the Sydney airport for the corresponding month and year [21]. Figure 1 shows the load and temperature profiles as well as their mean and variance across the month. Note that the battery is assumed to be installed outside and subjected to the ambient temperature and no direct solar radiation.

The TOU rate and demand charge are taken from [22]. The TOU rate has a price ratio of about 1-to-5, which is larger than most TOU rates [23]. The demand charge uses 30-minute average demand and, in our formulation, is not restricted to the on-peak period. Battery electrical parameters were taken or derived from [24]–[27]. We assume the battery is AC-coupled, and do not consider inverter power limits. Thermal parameters were derived from [5], [26], and [27]. Other values were estimated using the previous sources to achieve reasonable values for a typical residential battery.

The controller performance was assessed using the cost function from Equation (9). To determine the actual cost to the customer across the entire month, we replace n_k with the total number of time steps throughout the simulation, use the actual total power $P_{\text{tot},k}$ instead of $\overline{P}_{\text{tot},k}$, and set $\sigma_{P_{\text{load}}} = 0$.

A. MPC Reference Scenarios

Reference scenarios are run using a MPC framework similar to the proposed framework in Section II. Equation (13) is used for the MPC framework with all variance parameters (σ_{T_a}, $\sigma_{P_{\text{load}}}$, and σ_{T_b}) set to zero. The Perfect Forecast scenario

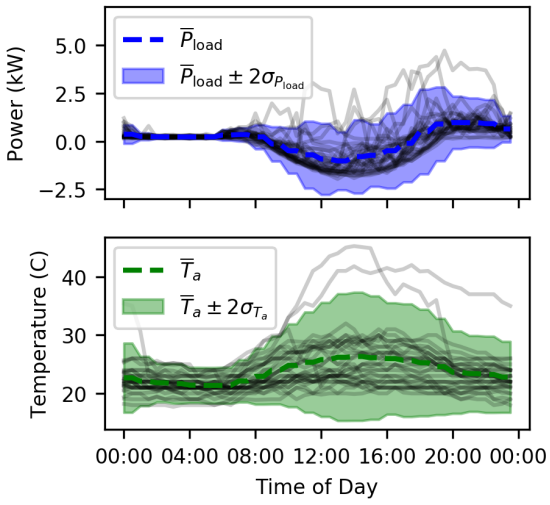

Fig. 1. Daily Profiles for (a) Customer Load P_{load} and (b) Ambient Temperature T_a for each day of simulation. Shaded region shows $\overline{z} \pm 2\sigma_z$.

uses the exact load and temperature as the forecasts for the MPC optimization. The MPC Baseline uses the same forecast as the SMPC Baseline scenario.

Table II shows the results of all the scenarios. The TOU and demand costs are taken from the first two terms in Equation (9), and other costs include costs due to degradation. As expected, the MPC with a perfect forecast performs very well, significantly lowering the total cost. The baseline MPC run performs poorly, especially considering the demand charge cost, since there are significant deviations between the baseline forecast and the actual power.

B. Baseline Scenario

The SMPC Baseline scenario uses the mean and variance of the load and temperature profiles calculated on an hourly basis as shown in Figure 1. Note that the $\overline{z} \pm 2\sigma_z$ interval contains the majority of the data, although a few days of the month have very high powers and high temperatures. The two days with the largest load correspond to the two days with the highest temperatures.

The controller successfully reduces the total cost to the customer across the month from $19.94 (from the MPC Baseline scenario) to $15.01 as shown in Table II. This improvement primarily comes from a reduction in peak demand that is enabled by the controller's load forecast. The TOU cost increased slightly, likely due to the focus of the SMPC control on the demand charge; for example, if there is a risk of approaching the peak power, the controller will reduce the chance of exceeding it by discharging more or charging less, even if that leads to increased TOU costs.

Figure 2 shows the results of the baseline scenario for the peak load day of the month. The battery charged during nighttime hours when electricity prices are low and uncertainty in load is low. It waits to discharge the battery until about 16:00 during the on-peak period, which is about when the load power increases and becomes more variable. It successfully lowered the peak demand before 20:00. However, the controller did

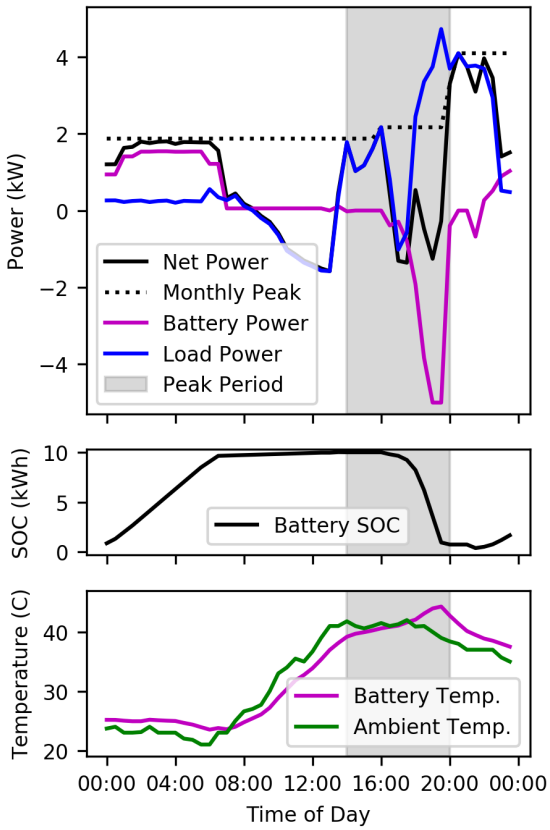

Fig. 2. Results for SMPC Baseline Scenario on the Peak Load Day

not expect the load power to remain high after 20:00, and it almost fully discharged during the on-peak period. Right after 20:00, the battery stopped discharging and the net load increased dramatically, which led to a large increase in the peak power, and the largest peak of the month.

The baseline controller had no information about the high demand or high temperature of this day; it was only provided the expected value and variance shown in Figure 1. Therefore, it could not have predicted the high load power, nor the high ambient temperature late in the day.

The simulation ran in 45 seconds, or 31 ms per time step, on a Dell PC with a 1.9 GHz Intel Core i7 processor and 16 GB of RAM. The simulation is run in Python with a publicly available convex optimization solver [28].

C. Effect of Risk

One method to improve the performance of the baseline controller is to increase the risk tolerance for high peak demand and high battery temperatures by decreasing the back-off magnitudes ζ_P and ζ_T. Decreasing ζ_P will decrease the value of the 2nd term in Equation (9) for time steps when there is a risk of exceeding the previous peak demand, leading to more charging or less discharging when the load is estimated to be high or is more uncertain. Decreasing ζ_T will loosen the constraint on $\overline{T}_{b,k}$ through Equation (11), which will increase the battery charge and discharge power when the battery temperature is close to $T_{\max}$. Both of these changes will make

the controller behave more aggressively during times when the load power and the ambient temperature is high.

We run the controller with High Risk conditions $\zeta_P = 1.28$ and $\zeta_T = 1.28$, corresponding to the 90$^{\text{th}}$ percentile of a Gaussian distribution. The performance results are shown in Table II and are slightly improved over the SMPC baseline scenario. The more aggressive control was able to reduce the TOU cost without increasing the demand charge cost. The peak time and day was the same for this scenario and for the baseline scenario.

We note that lower risk tolerance and more aggressive control behavior will not improve performance in all instances. The nature of the data used in these scenarios, and in particular the load profile on the peak day, cause the higher risk scenarios to lower the total costs.

D. Effect of Uncertainty

A preferable method to improve the controller performance, when possible, is to provide a more accurate prediction of load and temperature forecasts to the controller. Using the monthly load data and a publicly available model estimation tool, we develop an autoregressive (AR) model of the load power to reduce the uncertainty of the load forecast [29]. While more complex methods can create more accurate forecasts [30], we chose a first order AR model for simplicity. The load power is estimated as:

$$\begin{aligned} P_{\text{load},k} &= \overline{P}_{\text{load},k} + P_{\text{AR},k} \\ P_{\text{AR},k} &= 0.7977 P_{\text{AR},k-1} + \epsilon_{\text{AR},k} \end{aligned} \tag{14}$$

where $P_{\text{AR},k}$ is the difference between the actual load power and the mean load power. The mean load power $\overline{P}_{\text{load},k}$ is the same as in the original formulation, but the variance of $P_{\text{load},k}$ is now defined by $\epsilon_{\text{AR},k} \sim \mathcal{N}(0, \sigma^2_{P_{\text{AR},k}})$. We note that $\sigma_{P_{\text{AR},k}} < \sigma_{P_{\text{load},k}}$ for all hours of the day.

The AR Model scenario reduces total cost relative the the previous SMPC scenarios. Table II shows the TOU cost increases while the demand cost decreases. The improved demand forecast allows the controller to predict high consumption in the future, which greatly reduces the peak demand and the demand cost. It is likely that the conservative back-off parameter ζ_T causes the controller to reduce discharge power during the hot afternoons, which then increases the TOU cost since that is when the on-peak period occurs.

The final scenario tests the AR model with a higher risk tolerance. The combination of these effects lowers the total cost to $9.56 for the month. The addition of higher risk and more aggressive controls leads to lower TOU costs and higher demand costs.

Figure 3 shows the results of the scenario with the AR model and a higher risk tolerance for the peak load day of the month. Compared to the SMPC baseline scenario, the battery discharges more slowly during the on-peak period to conserve battery charge. It is able to more closely follow the peak power and limit the peak power increase during the peak period. It is also able to keep the battery temperature lower than the baseline SMPC controller did. The peak power still achieves its maximum value around 22:00, but at a lower value than in previous scenarios.

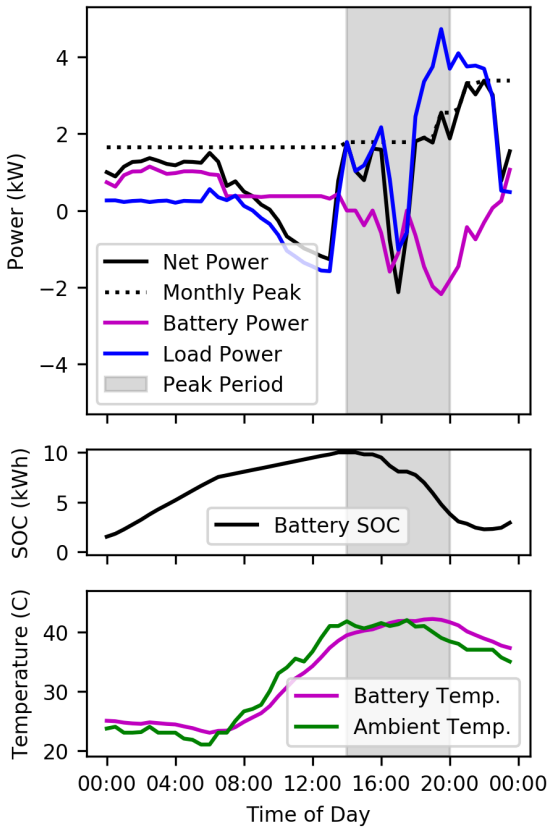

Fig. 3. Results for SMPC Scenario with AR Model and High Risk Tolerance on the Peak Load Day

TABLE II. PERFORMANCE RESULTS FOR ALL SCENARIOS

Scenario	TOU Cost	Demand Cost	Other Costs	Total Cost
No Battery	$-2.01	$40.47	$0	$38.47
Perfect Forecast	$-26.62	$14.74	$10.81	$-1.07
MPC Baseline	$-33.20	$41.64	$11.50	$19.94
SMPC Baseline	$-31.17	$35.07	$11.10	$15.01
SMPC, High Risk	$-32.89	$35.07	$11.23	$13.41
SMPC, AR Model	$-23.62	$25.96	$10.49	$12.83
AR + High Risk	$-30.65	$29.52	$10.69	$9.56

IV. CONCLUSION

In this paper, we formulate a thermo-electric battery model and a stochastic MPC controller that optimizes battery cycling over a TOU and demand charge rate structure. The controller accounts for uncertainty in the load forecast and ambient temperature forecast, maintains low battery temperatures, and maintains low charge and discharge rates to minimize the effects of degradation. Simulation results show that all SMPC scenarios perform better than the MPC when there is uncertainty in the forecast. We show that reducing forecast uncertainty improves the performance of the SMPC controller. Increasing risk tolerance to force a more aggressive control strategy also improves performance, although that result may not be generalizable to other scenarios.

There are many research topics to explore in the area of stochastic MPC for stationary batteries and other behind-the-meter devices. Using more advanced forecasting models, including temperature forecasting, would further reduce the

model uncertainty and should improve the control performance. More accurate battery models can be used, especially for understanding the impact on battery degradation. New controllers can optimize over different rate structures, for example using tiered rates, having demand charges that vary by time of day, and requiring the battery to only charge from on-site solar generation. The SMPC framework can also be coupled with additional methods for state estimation, parameter estimation, and other controllers such as a real-time battery controller, other device controllers, or a building-level management system.

ACKNOWLEDGMENT

This work was authored in part by the National Renewable Energy Laboratory, operated by Alliance for Sustainable Energy, LLC, for the U.S. Department of Energy (DOE) under Contract No. DE-AC36-08GO28308. Funding provided by U.S. Department of Energy Office of Energy Efficiency and Renewable Energy. The views expressed in the article do not necessarily represent the views of the DOE or the U.S. Government. The U.S. Government retains and the publisher, by accepting the article for publication, acknowledges that the U.S. Government retains a nonexclusive, paid-up, irrevocable, worldwide license to publish or reproduce the published form of this work, or allow others to do so, for U.S. Government purposes.

REFERENCES

[1] GTM Research and ESA, "U.S. Energy Storage Monitor," Tech. Rep., 2016. [Online]. Available: https://www.woodmac.com/research/products/power-and-renewables/us-energy-storage-monitor/

[2] IRENA, "Innovation landscape brief: Utility-Scale Batteries innovation Landscape Brief," Tech. Rep., 2019. [Online]. Available: www.irena.org

[3] P. P. Mishra, A. Latif, M. Emmanuel, Y. Shi, K. McKenna, K. Smith, and A. Nagarajan, "Analysis of degradation in residential battery energy storage systems for rate-based use-cases," *Applied Energy*, vol. 264, p. 114632, apr 2020. [Online]. Available: https://linkinghub.elsevier.com/retrieve/pii/S0306261920301446

[4] K. Smith, Y. Shi, and S. Santhanagopalan, "Degradation mechanisms and lifetime prediction for lithium-ion batteries - A control perspective," in *Proceedings of the American Control Conference*, vol. 2015-July. Institute of Electrical and Electronics Engineers Inc., jul 2015, pp. 728–730.

[5] L. H. Saw, Y. Ye, and A. A. Tay, "Electro-thermal analysis and integration issues of lithium ion battery for electric vehicles," *Applied Energy*, vol. 131, pp. 97–107, oct 2014.

[6] E. Raszmann, K. Baker, Y. Shi, and D. Christensen, "Modeling stationary lithium-ion batteries for optimization and predictive control," in *2017 IEEE Power and Energy Conference at Illinois, PECI 2017*. Institute of Electrical and Electronics Engineers Inc., may 2017.

[7] N. Diorio, "An Overview of the Automated Dispatch Controller Algorithms in the System Advisor Model," no. November, p. 22, 2017. [Online]. Available: www.nrel.gov/publications. https://www.nrel.gov/docs/fy18osti/68614.pdf

[8] X. Lin *et al.*, "A lumped-parameter electro-thermal model for cylindrical batteries," *J. Power Sources*, vol. 257, pp. 1–11, 2014. [Online]. Available: http://dx.doi.org/10.1016/j.jpowsour.2014.01.097

[9] H. E. Perez, X. Hu, S. Dey, and S. J. Moura, "Optimal Charging of Li-Ion Batteries with Coupled Electro-Thermal-Aging Dynamics," *IEEE Transactions on Vehicular Technology*, vol. 66, no. 9, pp. 7761–7770, sep 2017.

[10] J. Giraldez *et al.*, "Advanced Inverter Voltage Controls: Simulation and Field Pilot Findings," no. October, 2018. [Online]. Available: https://www.nrel.gov/docs/fy19osti/72298.pdf

[11] K. Garifi, K. Baker, D. Christensen, and B. Touri, "Control of Energy Storage in Home Energy Management Systems: Non-Simultaneous Charging and Discharging Guarantees," apr 2018. [Online]. Available: http://arxiv.org/abs/1805.00100

[12] B. Suthar *et al.*, "Optimal control and state estimation of lithium-ion batteries using reformulated models," in *American Control Conference (ACC), 2013*. IEEE, 2013, pp. 5350–5355.

[13] V. T. Dao, H. Ishii, and Y. Hayashi, "HEMS Operation with Utility Requirements for Rooftop Solar-Battery Systems," in *IEEE Power and Energy Society General Meeting*, vol. 2018-Augus. IEEE Computer Society, dec 2018.

[14] T. A. N. Heirung, J. A. Paulson, J. O'Leary, and A. Mesbah, "Stochastic model predictive control — how does it work?" *Computers and Chemical Engineering*, vol. 114, pp. 158–170, jun 2018.

[15] A. Hooshmand, M. H. Poursaeidi, J. Mohammadpour, H. A. Malki, and K. Grigoriads, "Stochastic model predictive control method for microgrid management," in *Innovative Smart Grid Technologies (ISGT), 2012 IEEE PES*. IEEE, 2012, pp. 1–7.

[16] S. R. Cominesi, M. Farina, L. Giulioni, B. Picasso, and R. Scattolini, "A Two-Layer Stochastic Model Predictive Control Scheme for Microgrids," *IEEE Transactions on Control Systems Technology*, vol. 26, no. 1, pp. 1–13, jan 2018.

[17] S. Park and C. Ahn, "Stochastic model predictive controller for battery thermal management of electric vehicles," in *2019 IEEE Vehicle Power and Propulsion Conference, VPPC 2019 - Proceedings*. Institute of Electrical and Electronics Engineers Inc., oct 2019.

[18] R. Kumar *et al.*, "A Stochastic Model Predictive Control Framework for Stationary Battery Systems," *IEEE Transactions on Power Systems*, vol. 33, no. 4, pp. 4397–4406, jul 2018.

[19] R. E. Kalman, "A new approach to linear filtering and prediction problems," *Journal of Fluids Engineering, Transactions of the ASME*, vol. 82, no. 1, pp. 35–45, mar 1960.

[20] "Solar home electricity data - Ausgrid." [Online]. Available: https://www.ausgrid.com.au/Industry/Our-Research/Data-to-share/Solar-home-electricity-data

[21] H. J. Diamond *et al.*, "U.S. Climate Reference Network after One Decade of Operations: Status and Assessment," *Bulletin of the American Meteorological Society*, vol. 94, no. 4, pp. 485–498, apr 2013. [Online]. Available: http://journals.ametsoc.org/doi/abs/10.1175/BAMS-D-12-00170.1

[22] S. Ann Abraham, K. McKenna, and A. Nagarajan, "Development and Clustering of Rate-Oriented Load Metrics for Customer Price-Plan Analysis," in *IEEE Power and Energy Society General Meeting*, vol. 2019-Augus. IEEE Computer Society, aug 2019. [Online]. Available: https://www.nrel.gov/docs/fy19osti/72655.pdf.

[23] R. Hledik, A. Faruqui, and C. Warner, "The National Landscape of Residential TOU Rates: A Preliminary Summary," The Brattle Group, Tech. Rep., 2017.

[24] "Public Report 6 Lithium Ion Battery Testing," ITP Renewables, Tech. Rep., 2019. [Online]. Available: www.batterytestcentre.com.au

[25] J. Svarc, "Tesla Powerwall 2 Vs LG chem RESU Vs Sonnen ECO Vs BYD — Clean Energy Reviews," 2019. [Online]. Available: https://www.cleanenergyreviews.info/blog/powerwall-vs-lg-chem-vs-sonnen-vs-byd

[26] LG Chem, "LG Home Battery." [Online]. Available: https://www.lgessbattery.com/us/home-battery/product-info.lg

[27] "Tesla Powerwall," Tech. Rep.

[28] S. Diamond and S. Boyd, "CVXPY: A Python-embedded modeling language for convex optimization," *Journal of Machine Learning Research*, vol. 17, pp. 1–5, 2016. [Online]. Available: http://www.cvxpy.org/

[29] S. Seabold and J. Perktold, "Statsmodels: Econometric and Statistical Modeling with Python," in *Proc. of the 9th Python in Science Conf*, no. Scipy, 2010, pp. 92–96. [Online]. Available: http://statsmodels.sourceforge.net/

[30] X. Li and J. Wen, "Review of building energy modeling for control and operation," pp. 517–537, sep 2014.